Neuropsychopharmacology (2015) 40, 2015–2024

www.neuropsychopharmacology.org

Integrin β3 Haploinsufficiency Modulates Serotonin Transport and Antidepressant-Sensitive Behavior in Mice

Matthew Mazalouskas[1,6], Tammy Jessen[1,6], Seth Varney[1], James S Sutcliffe[2,3], Jeremy Veenstra-VanderWeele[4], Edwin H Cook Jr[5] and Ana MD Carneiro*[,1]

[1]Department of Pharmacology, Vanderbilt University School of Medicine, Nashville, TN, USA; [2]Department of Psychiatry, Vanderbilt University School of Medicine, Nashville, TN, USA; [3]Department of Molecular Physiology and Biophysics, Vanderbilt University School of Medicine, Nashville, TN, USA; [4]Department of Psychiatry, Columbia University, New York City, NY, USA; [5]Department of Psychiatry, University of Illinois at Chicago, Chicago, IL, USA

Converging lines of evidence have identified genetic interactions between the serotonin transporter (SERT) gene and *ITGB3*, which encodes the β3 subunit that forms the αIIbβ3 and αvβ3 integrin receptor complexes. Here we examine the consequences of haploinsufficiency in the mouse integrin β3 subunit gene (*Itgb3*) on SERT function and selective 5-hydroxytryptamine (5-HT) reuptake inhibitor (SSRI) effectiveness *in vivo*. Biochemical fractionation studies and immunofluorescent staining of murine brain slices reveal that αvβ3 receptors and SERTs are enriched in presynaptic membranes from several brain regions and that αvβ3 colocalizes with a subpopulation of SERT-containing synapses in raphe nuclei. Notably, we establish that loss of a single allele of *Itgb3* in murine neurons is sufficient to decrease 5-HT uptake by SERT in midbrain synaptosomes. Pharmacological assays to elucidate the αvβ3-mediated mechanism of reduced SERT function indicate that decreased integrin β3 subunit expression scales down the population size of active SERT molecules and, as a consequence, lowers the effective dose of SSRIs. These data are consistent with the existence of a subpopulation of SERTs that are tightly modulated by integrin αvβ3 and significantly contribute to global SERT function at 5-HT synapses in the midbrain. Importantly, our screen of a normal human population for single nucleotide polymorphisms in human *ITGB3* identified a variant associated with reductions in integrin β3 expression levels that parallel our mouse findings. Thus, polymorphisms in human *ITGB3* may contribute to the differential responsiveness of select patients to SSRIs.
Neuropsychopharmacology (2015) **40,** 2015–2024; doi:10.1038/npp.2015.51; published online 11 March 2015

INTRODUCTION

Serotonin (also known as 5-hydroxytryptamine (5-HT)) plays important functional roles in the gastrointestinal tract, cardiovascular system, and the central nervous system (CNS). Dysfunctional 5-HT homeostasis and neurotransmission within the CNS has been associated with major depression, anxiety, obsessive-compulsive disorder, drug abuse, and autism-spectrum disorders (Cook and Leventhal, 1996; Ruhe *et al*, 2007). Used to treat depression and anxieties, selective 5-HT reuptake inhibitors (SSRIs) exert their neuromodulatory effects by binding to and inhibiting the function of the 5-HT transporter (also known as 5-HTT, SERT). SERT-mediated removal of extracellular 5-HT plays an important role in the repackaging of 5-HT into presynaptic vesicles and restricts the availability of 5-HT to activate pre- and post-synaptic 5-HT receptors (Blakely *et al*, 1998). Although the immediate effects of SSRI dosing include dramatic increases in extracellular 5-HT and activation of post-synaptic 5-HT receptors (Ramaiya *et al*, 1997), the therapeutic effects of SSRIs are associated with long-term exposure that includes desensitization of 5-HT auto-receptors and alterations in synaptic structure and function (Mayorga *et al*, 2001). Therefore, SSRI effectiveness depends on both proximal (eg, SERT and 5-HT receptors) and distal factors (eg, synaptic plasticity, synaptogenesis, and neurogenesis).

Blood 5-HT levels are utilized as an endophenotype for neuropsychiatric disorders in humans (DeLisi *et al*, 1981; Cook and Leventhal, 1996; Cleare, 1997; Askenazy *et al*, 1998; Verkes *et al*, 1998; Ma *et al*, 2007; Wulsin *et al*, 2009). The *ITGB3* gene, coding for the integrin *β*3 subunit, has been consistently identified as a quantitative locus for regulating whole blood 5-HT levels (Weiss *et al*, 2004, 2006a; Coutinho *et al*, 2007; Cross *et al*, 2008). The platelet integrin *α*IIb*β*3 receptor (also known as glycoprotein IIb/IIIa) was discovered to directly interact with SERT and modulate SERT-mediated uptake of extracellular 5-HT (Carneiro *et al*, 2008). A large family of obligatory, heterodimeric glycoproteins composed of an *α* chain and a *β* chain, integrin receptors mediate cell–cell/cell–matrix interactions and have

*Correspondence: Dr AMD Carneiro, Department of Pharmacology, Vanderbilt University School of Medicine, 461 Preston Research Building, 23rd Avenue South at Pierce, Nashville, TN 37232, USA, Tel: +1 615 875 5635, Fax: 615-343-1084,
E-mail: ana.carneiro@vanderbilt.edu
[6]These authors contributed equally to this work.
Received 20 August 2014; revised 6 February 2015; accepted 8 February 2015; accepted article preview online 16 February 2015

important functional roles in neurons regulating axon growth, guidance, and regeneration as well as synaptic structural changes associated with synaptic activity (Chavis and Westbrook, 2001; Milner and Campbell, 2002; Nikonenko *et al*, 2003; Pozzi and Zent, 2003; Cingolani *et al*, 2008). Recently, our laboratory examined the genetic interaction between the murine *Itgb3* and the SERT (*Slc6a4*) genes and identified a functional decrease in SERT-mediated 5-HT uptake in synaptoneurosomes from the midbrain and cortex, but not from the hippocampus, of $Itgb3^{+/-}$ mice (Whyte *et al*, 2014). This study implicates a conserved role for the integrin $\beta3$ subunit in the modulation of SERT function in the periphery and in the CNS, where the integrin $\beta3$ subunit associates with the integrin αv subunit to form the vitronectin receptor (ie, $\alpha v\beta3$).

Given the convergent evidence of the integrin $\beta3$ subunit in the modulation of serotonergic signaling, we examined the localization of integrin $\alpha v\beta3$ receptors and the mechanism(s) through which integrin $\alpha v\beta3$ receptors regulate SERT function in the midbrain. In this report, we demonstrate the expression of $\alpha v\beta3$ receptors in neurons within and outside of the raphe nuclei of the murine midbrain and their enriched localization to the presynaptic terminals of neurons within several brain regions. In the midbrain, $\alpha v\beta3$ receptors co-localize with a subpopulation of serotonergic synapses, which exhibit decreased 5-HT uptake in mice containing a heterozygous reduction in integrin $\beta3$ subunit expression. Assays to elucidate the integrin-mediated mechanism indicate that fewer molecules of SERT are active when $\alpha v\beta3$ receptor levels decrease. In support of this, $Itgb3^{+/-}$ mice, predicted to have a smaller population of active SERT, required a lower effective dose of SSRI in tail suspension tests (TSTs). Last, we identify a common polymorphism in human *ITGB3* that reduces integrin $\beta3$ subunit expression, suggesting that polymorphisms in human *ITGB3* can contribute to the differential responsiveness of select patients to SSRIs.

MATERIALS AND METHODS

Reagents

R/S citalopram hydrobromide, paroxetine hydrochloride hemihydrate, and 5-HT (5-hydroxytryptamine creatinine sulfate complex) were purchased from Sigma (St Louis, MO). Radioligands were purchased from PerkinElmer Life Sciences (Waltham, MA). Purified $\alpha v\beta3$ was purchased from Chemicon International (Millipore, Billerica, MA). Antibody sources: rabbit anti-mouse integrin $\beta3$ and PSD-95: Cell Signaling Technology (Denvers, MA); mouse anti-integrin αv: BD Biosciences (San Jose, CA); mouse anti-neuronal nuclei (NeuN), SNAP25, synaptophysin, and NMDAR: Chemicon International; guinea-pig anti-SERT: Frontier Science (Hokkaido, Japan).

Animals

Mouse studies were performed in accordance with humane guidelines established by the Vanderbilt Institutional Animal Care and Use Committee (IACUC) under approved protocols (M/12/167). Mice used in this study were males generated from $Itgb3^{+/+} \times Itgb3^{+/-}$ crosses originated from an *Itgb3* null line, provided by Dr Hynes at MIT (Hodivala-Dilke *et al*, 1999), which were backcrossed over 20 generations to C57BL/6. Mice were group-housed with their littermates and maintained on a 12-h light–dark cycle and provided with food and water *ad libitum*.

Immunofluorescence

Mice (9 $Itgb3^{+/+}$ and 4 $Itgb3^{-/-}$) were perfused with 30 ml 4% paraformaldehyde (Sigma). Brains were stored in 30% sucrose for 48 h at 4 °C, and then stereotaxically sectioned every 30 μm on a frozen stage microtome (Leica) and stored in a cryoprotectant solution (30% ethylene glycol, 30% glycerol in phosphate-buffered saline (PBS)). Sections collected between ~4 and 5 mm from Bregma were defined as midbrain sections. Immediately before use, serial sections were washed in tris-buffered saline (TBS). Slices were treated with Na^+/citrate solution (10 mM tri-sodium citrate dihydrate, pH 6.0 containing 0.05% Tween-20) at 50 °C for 5 min. Endogenous peroxidase was quenched by incubating sections in 1% H_2O_2 for 30 min. Slices were blocked with blocking buffer (1× TBS containing 5% goat serum, 1% bovine serum albumin, and 0.25% Triton X-100) for 1 h at room temperature. Primary antibodies were added at a 1 : 250 dilution in blocking buffer and incubated for 16 h at 4 °C. Integrin $\beta3$ signal was amplified by preincubating biotinylated anti-rabbit antibody with streptavidin-conjugated horseradish peroxidase (both diluted at 1 : 500 in blocking buffer) for 15 min at room temperature, followed by incubation with slices for 1 h at room temperature. After washing with 1× TBS, slices were incubated with tyramide solution (TSA Biotin Plus Tyramide Reagent; Perkin Elmer, CA) for 10 min. After washing with 1× TBS, fluorescent secondary antibodies (goat anti-mouse-Cy5, streptavidin-Cy2, and goat anti-guinea-pig-Cy3; Jackson ImmunoResearch Laboratories, West Grove, PA) were applied at a 1 : 500 concentration for 16 h at room temperature. Slices were washed in 1× TBS and mounted onto slides using Aqua-Poly/Mount (Polysciences, Warrington, PA). Wide field images were captured using a Nikon AZ 100 M microscope. Confocal images were captured using a 1 μm pinhole on a Zeiss LSM 510 Meta confocal and prepared using the LSM 5 Image Browser (Zeiss, Erie, PA). Z-series of 12–15 images from 0.125 μm optical slices were acquired using a DeltaVision OMX super resolution microscope (GE Healthcare, Issaquah, Washington). Reconstruction of 3D-SIM images and 3D modeling was performed using softWorX software. Image acquisition and analysis were performed in part through the use of the VUMC Cell Imaging Shared Resource (supported by NIH grants CA68485, DK20593, DK58404, DK59637, and EY08126).

Isolation of Presynaptic Membranes

Synaptoneurosomes and membrane fractions were prepared as described previously (Phillips *et al*, 2001). In brief, mouse tissue was homogenized in 0.32 M sucrose containing 0.1 mM $CaCl_2$ and 1 mM $MgCl_2$ using a Teflon-glass tissue homogenizer (Wheaton Instruments, Millville, NJ). The homogenized tissue was centrifuged at 1000 *g* for 10 min at 4 °C and synaptoneurosomes collected by centrifugation at 10 000 *g* for 10 min at 4 °C. Synaptoneurosomes were lysed and non-synaptic proteins extracted by resuspending pellets in 20 mM Tris-HCl (pH 6.0 containing 0.1 mM $CaCl_2$, 1 mM

$MgCl_2$, and 0.1% Triton X-100) and immediate centrifugation at 100,000 *g* for 30 min at 4 °C. The pellet was then solubilized in 20 mM Tris-HCl (pH 8.0 and 1% Triton X-100) and incubated on ice for 15 min to extract presynaptic proteins. Postsynaptic proteins were separated by centrifugation at 10 000 *g* for 30 min at 4 °C and solubilized in Laemmli buffer for western blot analysis.

Synaptosomal Uptake and Binding Measures

Saturation kinetic and competition analyses of 5-HT uptake were performed on crude synaptosomal pellets prepared after homogenization in 0.32 M sucrose with 4 mM HEPES, pH 7.4 to remove post-synaptic membranes. The synaptosomal pellet was resuspended in uptake buffer (1 × KRH (130 mM NaCl, 1.3 mM KCl, 2.2 mM $CaCl_2$, 1.2 mM $MgSO_4$, and 1.2 mM KH_2PO_4) containing 1.8 g/L glucose, 10 mM HEPES, 100 μM pargyline, and 100 μM ascorbic acid). For saturation analysis, we incubated 25 μg of synaptosomes with increasing concentrations of 5-HT (12.5–400 nM) for 10 min at 37 °C. Uptake was terminated by filtration through polyethyleneimine-coated GF/B Whatman filters using a Brandel Cell Harvester (Brandel, Gaithersburg, MD). Filters were washed three times with ice-cold 1 × KRH buffer and immersed in scintillation liquid for 8 h before quantification of accumulated radioactivity by scintillation spectrometry (Beckman Coulter, Fullerton, CA). Counts obtained from the filtered samples were corrected for nonspecific uptake using parallel samples incubated at 37 °C with 1 μM paroxetine. Data from different experiments were combined by normalizing each $Itgb3^{+/-}$ curve to its corresponding $Itgb3^{+/+}$ control, where the data point at 100 nM 5-HT was considered 100%. Competition binding assays to assess 5-HT potency for [^{3}H]MPP^+ uptake or SSRI potency for inhibition of [^{3}H]5-HT uptake were performed as described in Henry *et al*, (2006). In brief, 25 μg synaptosomes were preincubated at 37 °C in a shaking water bath with increasing concentrations of competitor (1 pM–1 mM). After 10 min, 20 nM of the radiolabeled substrate was added, and samples incubated at 37 °C for an additional 10 min. Data were analyzed by using one-site competition binding parameters to calculate IC_{50} values.

We quantified the binding of the high affinity cocaine analog [^{125}I]RTI-55 (5 nM) to intact crude synaptosomes (25 μg) and binding of [^{3}H] 5-HT (20 nM) to presynaptic membranes at 4 °C for 20 min in modified PBS (pH 7.4, containing 0.1 mM $CaCl_2$ and 1.0 mM $MgCl_2$) in the presence or absence of a membrane-permeant (1 μM paroxetine) or membrane-impermeant (100 μM 5-HT) displacer, defining total and surface-specific binding, respectively (Zhu *et al*, 2004, 2006). To perform saturation analysis of [^{3}H] citalopram binding, crude synaptosomal pellets (~50 μl) were resuspended in 10 volumes of water with protease inhibitors and then equilibrated to 50 mM Tris, pH 7.4. After a 20 min incubation with rotation at 4 °C, samples were spun 15 000 *g* for 25 min at 4 °C. Pellets containing purified plasma membranes were resuspended in binding buffer (50 mM Tris, pH 7.4, 120 mM NaCl, and 5 mM $MgCl_2$). Purified membranes (43 μg), preincubated in the absence or presence of 1 μM paroxetine for 30 min at 4 °C, were incubated with increasing concentrations of [^{3}H] citalopram (0.625–100 nM) for 20 min at 4 °C. Binding was terminated by filtration as described above. All binding experiments were performed in duplicates using four or more mice.

Tail Suspension Test

An automated TST device (Med Associates, St Albans, VT) was used to measure the duration of behavioral immobility. Mice were suspended by the tail with tape to a vertical aluminum bar connected to a strain gauge. Before attaching the tail to the bar, each mouse had its tail passed through a clear 3 cm plastic tube to prevent mice from climbing their own tails. The following settings were used in all experiments: threshold 1: 7; gain: 8; time constant: 0.25; and resolution: 200 ms. Citalopram was prepared fresh daily by dissolving the powder in deionized water and diluted in 0.9% saline. Drug was administered by intraperitoneal injection in a volume of 0.01 ml/g body weight and the dose was 0, 2, 5, or 10 mg/kg calculated as the weight of the base. Each mouse was tested four times in the TST, with 1 week between testings. A counterbalanced design was used, where half of the animals of each genotype received citalopram in one order and the other half followed another order. No effects of multiple testing were observed. Mice were injected with drug or saline 30 min before a 6 min TST. A second cohort of mice was used to test immobility responses to paroxetine. In this cohort, mice received saline or paroxetine (5 mg/kg) via intraperitoneal injection and were then tested in the TST after 30 min. Data was analyzed by two-way ANOVA over the 6-min period (drug × genotype).

Western Blot of Human Platelet Samples

Human blood of *ITGB3* genotyped subjects was collected under an approved institutional review board protocol (the University of Illinois at Chicago) (Hammock *et al*, 2012). All subjects provided informed consent for research studies. Whole blood was collected and frozen at − 80 °C for shipping and analysis at Vanderbilt. Samples were thawed and resuspended in 1 ml H_2O for lysis of red blood cells. The remaining platelets were collected by centrifugation at 15 000 *g* for 30 min and washed 2 × with 1×PBS. Platelets were counted in a hemacytometer. Protein was extracted in 1% sodium dodecyl sulfate in PBS pH 7.4 containing protease inhibitor cocktail (containing AEBSF, aprotinin, bestatin, E-64, leupeptin, and pepstain A; Sigma-Aldrich, Saint Louis, MO). Protein was measured using a modified Lowry protocol with bicinchoninic acid (BCA Protein Assay Kit, Pierce Chemical Company, Rockford, IL). Protein extracts (25 μg) were submitted to SDS–PAGE and western blot analysis with chemiluminescence. Amersham Hyperfilm ECL films were exposed at 1, 5, 10, and 30 min to address linearity of the data (GE Healthcare, Pittsburgh, PA). Films were scanned in tagged image file format (.tiff) and bands quantified by densitometry using ImageJ. Data is presented as raw values normalized to the mean of the most common genotype. Gaussian distribution of the data was examined by D'Agostino & Pearson omnibus normality test. Data was analyzed using one-way ANOVA (for normally distributed data) or Kruskal–Wallis test (non-parametric analysis), when necessary. Dunn's multiple comparisons test was performed when appropriate, comparing the mean rank of each

genotype with the mean rank of all other genotypes, with each *P*-value adjusted for multiple comparisons ($\alpha = 0.05$). Allele frequencies in our data set were compared with dbSNP frequencies as reported in Table 1.

Data Analyses

All data was analyzed using GraphPad Prism software (Prism 6, GraphPad software, LaJolla, CA). Michaelis–Menten curve fit as a function of ligand concentration revealed K_m and V_{max} values in uptake and K_d and B_{max} in binding experiments, respectively. Statistical analyses are described in the figure legends.

RESULTS

Integrin αvβ3 Is Expressed in Raphe Neurons

To establish a role for integrin αvβ3 receptors in the modulation of SERT function in the CNS, we first examined the cellular distribution of integrin αvβ3 receptors within the murine midbrain by immunofluorescent staining. Given that the αv subunit can associate with other integrin β subunits (including β1, β5, β6, and β8), but the β3 subunit is restricted in its association with the αv subunit in the CNS, we utilized integrin β3 subunit specific antibodies to label αvβ3 receptors in midbrain slices of brains isolated from *Itgb3*$^{+/+}$ and *Itgb3*$^{-/-}$ littermates. Co-staining *Itgb3*$^{+/+}$ midbrain slices (Bregma −4.60 mm) with anti-integrin β3 and anti-NeuN antibodies revealed that αvβ3 receptors were expressed in neurons (Figure 1a). The integrin β3 subunit antibody failed to stain slices from *Itgb3*$^{-/-}$ mice, as well as *Itgb3*$^{+/+}$ slices preincubated with purified αvβ3, thus validating the specificity of this antibody (Figure 1b and data not shown). Further examination of integrin β3 subunit expression within serial sections of *Itgb3*$^{+/+}$ midbrains revealed that αvβ3 receptors were expressed in several regions, including the dorsal and median raphe nuclei where serotonergic neurons are located (Figure 1c).

Integrin αvβ3 Co-localizes with SERT in Adult Mouse Fibers

To examine the subcellular distribution of αvβ3 receptors in raphe neurons and their spatial relationship to SERT, we stained midbrain sections with antibodies recognizing the integrin β3 subunit, SERT, and the presynaptic marker synaptophysin. Using confocal microscopy, we observed integrin β3 subunit immunoreactivity in the cell bodies and fibers of neurons localized to the dorsal raphe, the latter of which also stained positive for SERT expression (Figure 2a1). We found that expression of SERT (SERT+) partially co-localized with expression of synaptophysin (Synapt+), indicating that some, but not all transporters were localized to presynaptic terminals. As indicated in the higher magnification image, populations of Synapt+/SERT+ puncta were identified where αvβ3 receptors were absent (Figure 2a2; letters a–c) or present (Figure 2a2; numbers 1–3). Employing structured illumination microscopy, we observed overlap of SERT and integrin β3 subunit signals on structures measuring ~0.150 μm (Figure 2b1,2,3). Three-dimensional reconstruction (Figure 2b4, Supplementary Movie) revealed co-localization of SERT and αvβ3 within organelles of ~1 μm diameter, consistent with the diameter of 5-HT synaptic terminals (arrow; Figure 2b5) (Arai *et al*, 2002) and at subcellular compartments of 0.1–0.2 μm along the fibers, possibly intracellular vesicles (arrowhead; Figure 2b7).

To further define the synaptic localization of integrin αvβ3 receptors in neurons, we utilized a pH-dependent solubility shift fractionation technique that allows for the separation of presynaptic active zones from post-synaptic densities (Phillips *et al*, 2001). Western analysis of fractions generated from cerebellum (Cb), midbrain (Mb), hippocampus (Hp), thalamus (Th), and striatum (St) demonstrated robust synaptic segregation, noted by the enrichment of the presynaptic protein synaptophysin alongside a relative exclusion of post-synaptic markers (NMDAR and PSD-95) in the presynaptic fractions (Figure 2c). Furthermore, these data revealed that αv and β3 subunits, together with SERT, were expressed in the presynaptic nerve terminals of several brain regions, including the midbrain (Figure 2c). Collectively, our studies suggest that two distinct populations of serotonergic synapses are present in the raphe and distinguished by co-localization of SERT with or without αvβ3 receptors.

Integrin β3 Haploinsufficiency Influences SERT-Mediated 5-HT Transport Velocity and Not Affinity

Data from our laboratory indicated that *Itgb3*$^{+/-}$ mice exhibit reduced midbrain 5-HT uptake activity (Whyte *et al*, 2014). Here, we utilized synaptosomal preparations, devoid of postsynaptic terminals, to elucidate the mechanism(s) by which αvβ3 receptors modulate SERT function. Synaptosomes isolated from the midbrains of *Itgb3*$^{+/-}$ mice expressed significantly lower levels of the integrin β3 subunit when compared with synaptosomes prepared from *Itgb3*$^{+/+}$ littermates (Figure 3a). No change in integrin αv subunit expression was observed. We assessed any genotype-specific differences in SERT function by collating and normalizing saturating curves from multiple 5-HT uptake experiments. As illustrated in the representative experiment, *Itgb3*$^{+/-}$ synaptosomes exhibited decreased uptake of 5-HT when compared with *Itgb3*$^{+/+}$ synaptosomes (Figure 3b). The pooled data demonstrated a 40% reduction in SERT-mediated 5-HT V_{max} and no change in the transporter's affinity (K_m) for 5-HT (Figure 3c and d). We also examined the ability of 5-HT to inhibit the uptake of 1-methyl-4-phenylpyridinium (also known as MPP^+) and observed no difference in 5-HT potency between genotypes (Figure 3e). In total, these data demonstrated that integrin αvβ3-mediated regulation of SERT 5-HT transport velocity can be modulated by changes in integrin β3 subunit expression.

Integrin αvβ3 Receptors Control Active SERT Population Numbers

Alterations in transporter expression, trafficking/recycling, and/or catalytic function could affect the kinetic properties of SERT and account for the decrease in V_{max} observed in *Itgb3*$^{+/-}$ synaptosomes. To evaluate if altered expression or trafficking/recycling rates of SERT were occurring, we performed radioligand displacement assays using [^{125}I]RTI-55 and SERT-selective lipophilic (ie, paroxetine) or hydrophobic (ie, 5-HT) competitors to define the total and plasma-

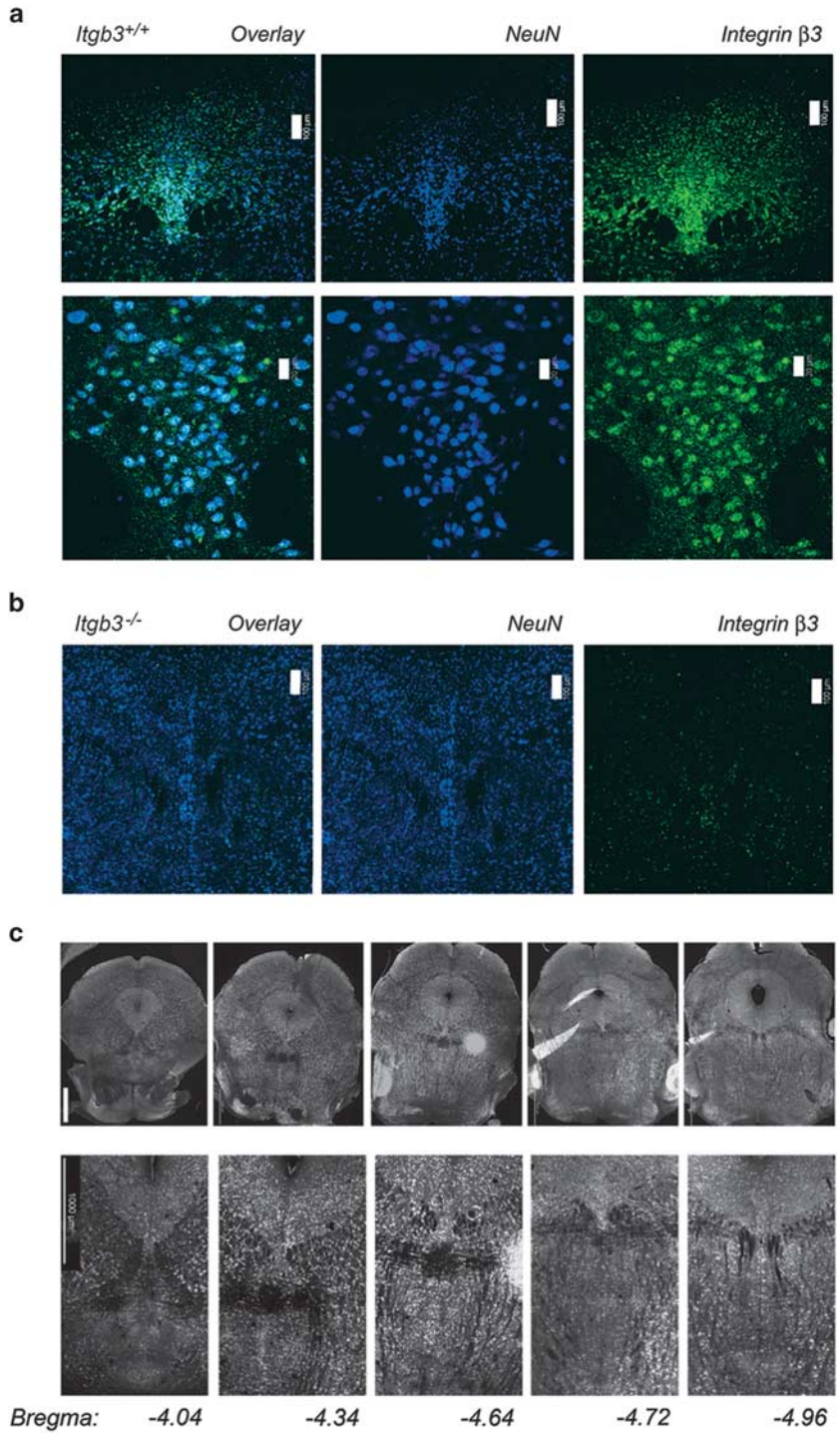

Figure 1 Integrin αvβ3 receptors are expressed in raphe neurons. (a and b) Representative images detailing the cellular localization of NeuN (blue) and integrin β3 subunit (green) together (Overlay) and individually in a midbrain slice (Bregma −4.60 mm), from an *Itgb3*$^{+/+}$ (a) or *Itgb3*$^{-/-}$(b) mouse, immunostained, and visualized using confocal microscopy. Magnification: ×20. Top panels in a and b, bar = 100 μm. Bottom panels in a, bar = 20 μm. (c) Immunofluorescent images of stereotaxic slices from an *Itgb3*$^{+/+}$midbrain stained for the integrin β3 subunit. Top panels: magnification: ×2.5. Bar = 1000 μm. Bottom panels: increased magnification of the dorsal and median raphe nuclei. Magnification: ×10. Bar = 1000 μm. Figures are representative images of $n = 3$ in each genotype. NeuN, neuronal nuclei.

membrane localized SERTs, respectively (Zhu *et al*, 2010). Both *Itgb3*$^{+/+}$ and *Itgb3*$^{+/-}$ synaptosomes were found to express similar levels of total and surface-bound SERT (Figure 4a). In parallel with our displacement assays, we biochemically isolated presynaptic plasma membrane fractions from midbrain synaptosomes and analyzed SERT expression by western blot. Consistent with our binding studies, no *Itgb3* genotype-dependent changes in SERT levels at the synaptic surface were observed (Figure 4b), suggesting that the reduced 5-HT uptake capacity in *Itgb3*$^{+/-}$ mice does not result from

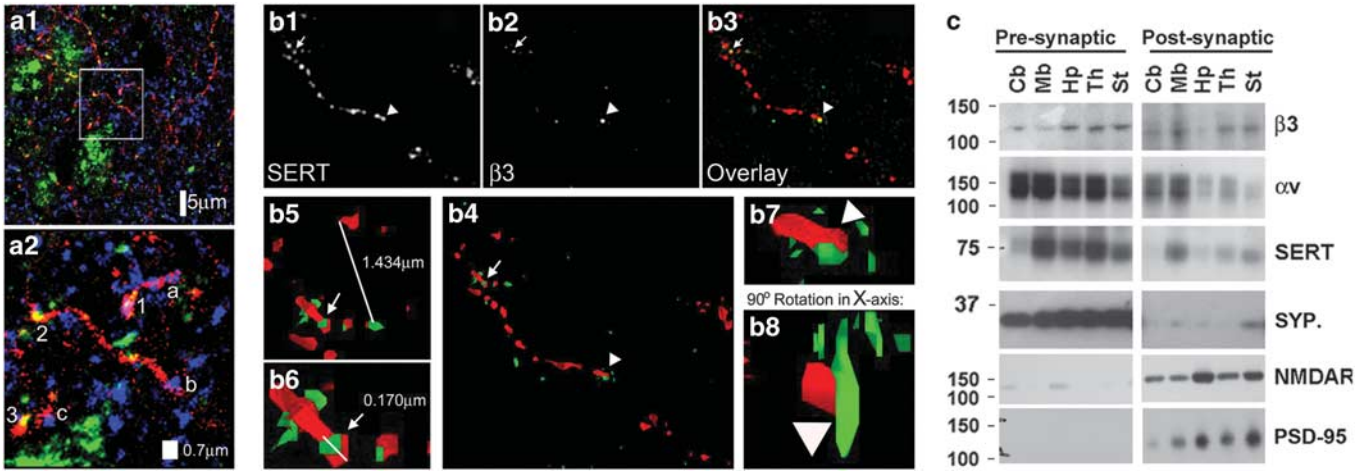

Figure 2 Integrin αvβ3 receptors partially co-localize with SERT in presynaptic terminals. (a1) Representative image detailing the distribution of synaptophysin (blue), SERT (red), and integrin β3 subunit (green) within dorsal raphe nucleus processes of an *Itgb3*$^{+/+}$ midbrain slice (Bregma −4.60 mm) immunofluorescently stained and visualized using confocal microscopy with a 1 μm pinhole. Optical Magnification: ×40. Bar = 5 μm. (a2) Magnification of the area in a1 outlined in white: Co-localization of synaptophysin and SERT identified serotonergic synapses that lacked (magenta; letters a–c) or expressed (yellow; numbers 1–3) αvβ3 receptors. Final digital magnification: ×100. Bar = 0.7 μm. (b) Analysis of a representative serotonergic neuron by structured illumination microscopy. (b1–3) Images of a neuron labeled for SERT (red) and integrin β3 subunit (green) individually and merged (Overlay) reveal two instances of protein co-localization (arrow and arrowhead). (b4) 3D reconstruction of the neuron in b1–3. (b5–6) Co-localization marked by the arrow in b4 occurs at a structure whose length of 1.434 μm is in agreement with consensus lengths of synapses. The width of the co-localized signal is 0.170 μm. (b7–8) Co-localization marked by the arrowhead in b4 occurs at another subcellular compartment, possibly an intracellular vesicle. Rotation of the co-localized signal in b7 by 90° in the *x*-axis (b8) highlights the proximity of the two signals to one another (see Supplementary Movie). Images shown are representative of 20 images of slices prepared from 5 *Itgb3*$^{+/+}$ mice. (c) Western blot analysis of cerebellum (Cb), midbrain (Mb), hippocampus (Hp), thalamus (Th), and striatum (St) synaptoneurosomes fractionated by a pH-dependent solubility shift technique into presynaptic active zones (pre-synaptic) and post-synaptic densities (post synaptic). Samples were analyzed using antibodies recognizing the integrin β3 and αv subunits, SERT, synaptophysin (SYP.), the NMDA receptor (NMDAR), and PSD-95. Data shown is representative of six independent experiments. SERT, serotonin transporter.

decreased expression of SERT or changes in the trafficking/recycling of SERT to the neuronal plasma membrane.

To delineate whether alterations in SERT catalytic function could explain the decrease in V_{max} in *Itgb3*$^{+/-}$ synaptosomes, we combined the 5-HT uptake data provided in Figure 3c with B_{max} estimates, derived from saturation [^{3}H] citalopram binding assays of purified plasma membranes, to estimate the 5-HT turnover rate for SERT in each genotype. The [^{3}H]citalopram binding curves shown in Figure 4c yielded turnover rates (ie, V_{max}/B_{max}) of 0.0064 and 0.0060 for SERT in *Itgb3*$^{+/+}$ and *Itgb3*$^{+/-}$, respectively. These data suggest that the catalytic function of active SERT molecules is similar in both genotypes.

One possible explanation for the observed reduction in V_{max} without diminishments in surface SERT levels or turnover rates is a decrease in the population of active SERT molecules. As our microscopy studies revealed the existence of two SERT populations distinguished by their co-localization with *αvβ3* receptors, we hypothesized that loss of integrin *β3* subunit expression inactivates a pool of *αvβ3*-associated SERTs. Given that the B_{max} values exhibited a strong trend toward a significant difference (Figure 4c), suggesting that fewer active SERTs were available to bind [^{3}H]citalopram, we examined the binding of [^{3}H]5-HT in presynaptic plasma membrane fractions. Analysis of these surface purified SERTs revealed a reduction in [^{3}H]5-HT binding in *Itgb3*$^{+/-}$ preparations (Figure 4d).

Based on our *ex vivo* findings, we predicted that a lower dose of SSRI would be effective in altering behaviors in mice in TST. The dose-response curve for acutely administered citalopram revealed that, while 10 mg/kg citalopram elicited decreases in immobility in the TST in both genotypes, 5 mg/kg produced a significant reduction in immobility in *Itgb3*$^{+/-}$ mice without affecting *Itgb3*$^{+/+}$ mice (Figure 4e). We found no significant genotype effects for basal immobility (Carter *et al*, 2011). Similar effects were observed in the TST when a second cohort of mice was exposed to 5 mg/kg paroxetine (Figure 4f). These changes do not appear to arise from altered *in vitro* potency of SSRIs to inhibit 5-HT transport, as both SSRIs displayed equivalent potency for SERT in synaptosomes from *Itgb3*$^{+/-}$ and wild-type littermates (Citalopram: *Itgb3*$^{+/+}$: Log_{IC50}: -8.21 ± 0.36, $n = 6$. *Itgb3*$^{+/-}$: Log_{IC50}: -8.13 ± 0.38, $n = 5$. Paroxetine: *Itgb3*$^{+/+}$: Log_{IC50}: -8.71 ± 0.16, $n = 5$. *Itgb3*$^{+/-}$: Log_{IC50}: -8.84 ± 0.16, $n = 5$). Taken together, our behavioral assays suggest that *αvβ3* receptors define a subpopulation of SERTs, which have high uptake capacity and may represent the main target of SSRIs.

Polymorphisms in Human *ITGB3* Affect Integrin *β3* Subunit Expression

Numerous functional polymorphisms within human *ITGB3* cause lack of (ie, <5% of normal) or reduced expression of (ie, 10–20% of normal) *α*IIb*β3* receptors on the platelet surface of patients with Glanzmann thrombasthenia (GT), a rare, heritable, or autoimmune coagulopathy (Nurden *et al*, 2011). Given our findings that a heterozygous reduction in integrin *β3* subunit expression reduces the effective dose of SSRIs to antagonize SERT, we performed a polymorphism

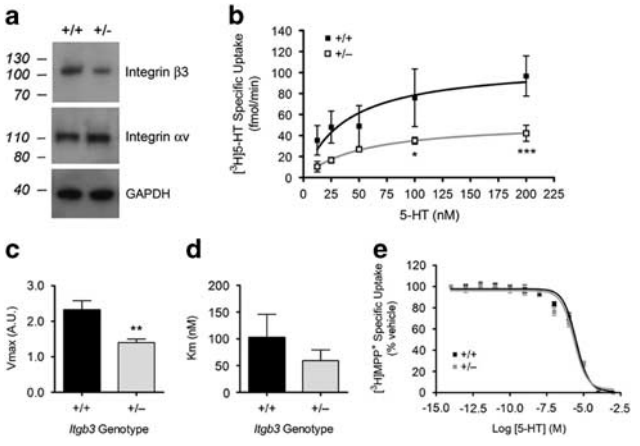

Figure 3 Integrin β3 haploinsufficiency decreases SERT function. (a) Western blot analysis of midbrain synaptosomes from *Itgb3*$^{+/+}$ and *Itgb3*$^{+/-}$ mice using antibodies recognizing the integrin β3 and αv subunits and GAPDH. Differences in integrin β3 subunit expression were significant when values in the *Itgb3*$^{+/-}$ condition were compared with *Itgb3*$^{+/+}$, which was set to 100. *Itgb3*$^{+/+}$ = 100 ± 0.5, n = 5; *Itgb3*$^{+/-}$ = 40.45 ± 14.7, n = 6. Unpaired t-test with Welch's correction: P = 0.009. Representative data from three independent experiments. (b) Representative kinetic saturation analysis experiment of [^{3}H] 5-HT specific uptake by SERT in *Itgb3*$^{+/+}$ (black) or *Itgb3*$^{+/-}$ (gray) midbrain synaptosomes. Two-way ANOVA Bonferroni post-test: *P < 0.05; ***P < 0.001. *Itgb3*$^{+/+}$, n = 4; *Itgb3*$^{+/-}$, n = 3. (c) Analysis of maximum SERT-mediated 5-HT transport velocity (V_{max}; arbitrary units (a.u.)) from pooled kinetic saturation experiments. *Itgb3*$^{+/+}$ = 2.322 ± 0.258, n = 13; *Itgb3*$^{+/-}$ = 1.402 ± 0.098, n = 15. Unpaired t-test with Welch's correction: P = 0.0045. (d) Analysis of SERT affinity for 5-HT (K_m) from pooled kinetic saturation experiments. *Itgb3*$^{+/+}$ = 102.4 ± 43.5, n = 13; *Itgb3*$^{+/-}$ = 59.4 ± 20.0, n = 15. Unpaired t-test with Welch's correction was non-significant. (e) Competition uptake curves for [^{3}H]1-methyl-4-phenylpyridinium ([^{3}H]MPP$^+$) with 5-HT in *Itgb3*$^{+/+}$ (black) or *Itgb3*$^{+/-}$ (gray) midbrain synaptosomes. *Itgb3*$^{+/+}$: Log_{IC50}: −5.528 ± 0.059, n = 4. *Itgb3*$^{+/-}$: Log_{IC50}: −5.655 ± 0.083, n = 4. Data presented as means ± SEM. ANOVA, analysis of variance; GAPDH, glyceraldehyde 3-phosphate dehydrogenase; HT, hydroxytryptamine; SERT, serotonin transporter.

screen in patients that do not have GT to identify single nucleotide polymorphisms (SNPs) in *ITGB3* that reduce integrin *β3* subunit expression. We tested for association of three common SNPs, rs2317385 (3475G > A, in the 5′UTR), rs15908 (42130 A > C, Val381Val, in exon 9), and rs12603582 (51370G > T, in intron 11), with altered platelet expression of the integrin *β3* subunit. Our findings revealed a significant reduction in integrin *β3* subunit protein levels in the CC homozygous genotype at rs15908 with no alteration in SERT or GAPDH expression (Table 1). We also observed significant reductions in integrin *β3* protein levels for the AA genotype of rs2317385, although this is likely driven by an extremely small sample size. For rs12603582, no statistically significant change in integrin *β3* subunit, SERT, or GAPDH expression was observed in patients carrying the minor allele (Table 1). These data suggest that the difference in integrin *β3* subunit expression in the haploinsufficient mouse is relevant to genetic variation in human patients without a coagulopathy.

DISCUSSION

Evidence documenting the association of *ITGB3* with whole blood 5-HT levels, replicated by multiple laboratories (Weiss

Table 1 Association of ITGB3 SNPs with Altered Expression Levels of Human Platelet Proteins.

SNP	Genotype	Minor allele frequency	Observed frequency (%)	N	Integrin β3				SERT				GAPDH			
					Mean ± SEM	AP test	Statistics[a] ANOVA		Mean ± SEM	AP test	Statistics ANOVA		Mean ± SEM	AP test	Statistics ANOVA	
rs2317385	GG	A = 30%/1505	72	49	100.0 ± 11.1	0.0258	Kruskal–Wallis	P = 0.0272	100.4 ± 6.8	0.2491	One-way ANOVA	P = 0.1018	100.9 ± 15.9	0.0028	Kruskal–Wallis	P = 0.4316
	GA		24	16	74.7 ± 10.7	0.4251			84.6 ± 9.4	0.1461			101.3 ± 20.9	< 0.0001		
	AA		4	3	13.9 ± 9.9*	N too small			48.31 ± 15.7	N too small			43.5 ± 32.3	N too small		
rs15908	AA	C = 43%/2159	49	33	100.7 ± 11.7	0.1172	Kruskal–Wallis	P = 0.0058	100.5 ± 7.4	0.5451	One-way ANOVA	P = 0.8861	100.3 ± 17.2	0.0193	Kruskal–Wallis	P = 0.2161
	AC		37	25	90.3 ± 15.0	0.0117			104.9 ± 11.8	0.4803			64.2 ± 14.9	0.0139		
	CC		15	10	37.0 ± 10.5**, #	0.1437			81.5 ± 11.1	0.2841			88.4 ± 28.1	> 0.1000		
rs12603582	GG	T = 15%/787	56	38	100.1 ± 14.7	0.0158	Kruskal–Wallis	P = 0.135	100.8 ± 7.4	> 0.1000	One-way ANOVA	P = 0.4437	100.2 ± 18.9	< 0.0001	Kruskal–Wallis	P = 0.4258
	GT		32	22	147.0 ± 21.8	0.0654			113.3 ± 13.8	> 0.1000			141.3 ± 23.2	0.0583		
	TT		12	8	124.1 ± 28.4	0.0498			112.0 ± 16.5	> 0.1000			46.2 ± 36.0	0.0565		

MAF: (Global minor allele frequency) dbSNP is reporting the minor allele frequency for each rs included in a default global population with the sample size for the MAF estimate listed after MAF.
[a]The statistical analysis of data was performed as follows: D'Agostino & Pearson omnibus normality test (P < 0.05 indicates that the data is not normally distributed). Analysis of variance (ANOVA) as indicated on the table. Post-tests were only performed when the ANOVA was significant (α = 0.05). Following Kruskal–Wallis test (P < 0.05), we performed Dunn's multiple comparison test comparing the mean rank of each column with the mean rank of every other column with P-values adjusted for multiple comparisons. *P < 0.05, **P < 0.01 *vs* common genotype and $^{\#}P$ < 0.05 *vs* heterozygous genotype.

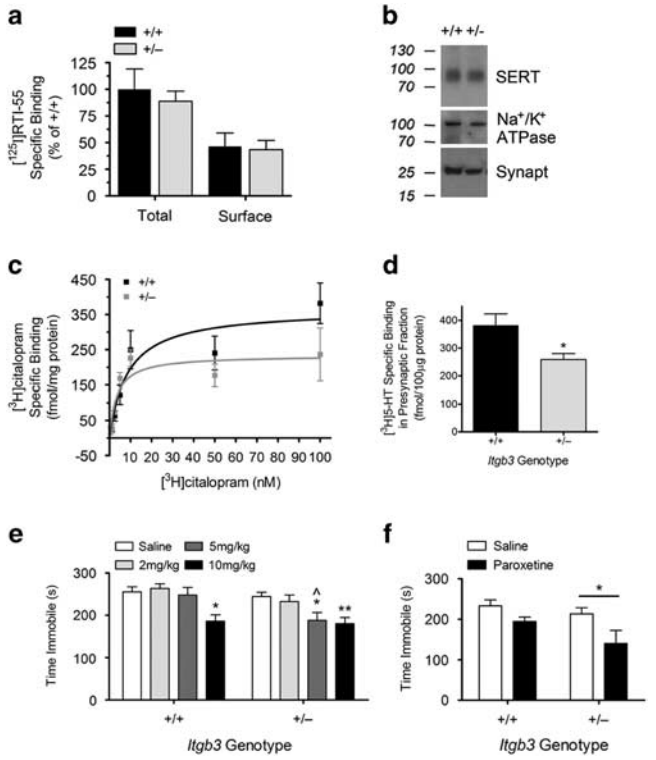

Figure 4 *Itgb3* haploinsufficiency decreases the number of active SERT molecules and effective SSRI dose. (a) Radioligand displacement assays using [^{125}I]RTI-55 identified levels of total SERT (Total) and plasma membrane-localized SERT (Surface) in the presence of excess paroxetine and 5-HT, respectively. $Itgb3^{+/+}$, $n=4$; $Itgb3^{+/-}$, $n=4$. (b) Representative western blot of purified presynaptic plasma membranes using antibodies recognizing SERT, Na^+/K^+-ATPase, and synaptophysin (Synapt). SERT values in the $Itgb3^{+/-}$ condition were compared with $Itgb3^{+/+}$: $Itgb3^{+/+} = 108.8 \pm 24.0$, $n=5$; $Itgb3^{+/-} = 117.1 \pm 16.1$, $n=5$. (c) Saturation analysis of [^{3}H]citalopram (0.625–100 nM) binding to presynaptic plasma membranes purified from $Itgb3^{+/+}$ (black) and $Itgb3^{+/-}$ (gray) synaptosomes. B_{max} $Itgb3^{+/+} = 365.2 \pm 42.69$, $n=3$; $Itgb3^{+/-} = 233.6 \pm 24.56$, $n=4$. Unpaired *t*-test with Welch's correction: $P=0.0761$. (d) Radioligand binding assays with 20 nM [^{3}H]5-HT were performed on $Itgb3^{+/+}$ (black) and $Itgb3^{+/-}$ (gray) presynaptic plasma membranes. $Itgb3^{+/+} = 381.3 \pm 41.96$, $n=7$; $Itgb3^{+/-} = 258.6 \pm 21.50$, $n=5$. Unpaired *t*-test with Welch's correction: $P=0.0315$. (e) Mice were administered saline or citalopram at doses of 2, 5, or 10 mg/kg and then the immobility times of animals in the tail suspension test were recorded. Asterisks represent drug effects within genotype comparisons: $^*P<0.05$ and $^{**}P<0.01$. Carrots represent genotype comparisons within each dose: $^\wedge P<0.05$. Saline: $Itgb3^{+/+} = 259.9 \pm 11.3$, $n=16$; $Itgb3^{+/-} = 244.4 \pm 10.0$, $n=23$. Two-way RM ANOVA citalopram effect: $F_{(3,148)} = 8.11$, $P<0.0001$. 5 mg/kg: $Itgb3^{+/+} = 248.6 \pm 14.6$, $n=16$; $Itgb3^{+/-} = 194.9 \pm 17.6$, $n=23$. Bonferroni post-test: $^*P=0.0246$, $^\wedge P=0.0358$. 10 mg/kg: $Itgb3^{+/+} = 183.2 \pm 14.2$, $n=16$; $Itgb3^{+/-} = 180.3 \pm 14.4$, $n=23$. Bonferroni post-test: $Itgb3^{+/+} = {}^*P=0.0417$, $Itgb3^{+/-} = {}^{**}P=0.0055$. (f) Mice were administered saline or 5 mg/kg paroxetine and then the immobility times of animals in the tail suspension test were recorded. $Itgb3^{+/+}{}_{saline} = 233.0 \pm 15.0$, $n=9$; $Itgb3^{+/+}{}_{paroxetine} = 194.7 \pm 10.6$, $n=6$; $Itgb3^{+/-}{}_{saline} = 213.6 \pm 15.0$, $n=9$; $Itgb3^{+/-}{}_{paroxetine} = 140.5 \pm 32.1$, $n=5$. Two-way ANOVA paroxetine effect $F_{(1,25)} = 9.29$, $P<0.005$. Bonferroni post-test: $Itgb3^{+/-}{}_{saline}$ *vs* $Itgb3^{+/-}{}_{paroxetine}$ $^*P=0.0220$. Data presented as means ± SEM. ANOVA, analysis of variance; HT, hydroxytryptamine; RM, repeated measures; SERT, serotonin transporter; SSRI, selective serotonin reuptake inhibitor.

et al, 2004, 2006a, 2006b; Coutinho *et al*, 2007; Cross *et al*, 2008; Napolioni *et al*, 2011) led us to examine whether haploinsufficiency in the integrin $\beta3$ gene modulates SERT function in the CNS. In contrast to studies in platelets, disruption of a single *Itgb3* allele in mice was sufficient to dramatically diminish 5-HT uptake by SERT in raphe synaptosomes, indicating that serotonergic signaling in the CNS is more sensitive to alterations in integrin $\beta3$ subunit expression (Carneiro *et al*, 2008). Assays to delineate the mechanism(s) behind the changes in SERT's kinetic properties revealed that integrin $\alpha v\beta3$ receptors play a permissive role in determining the number of active SERT molecules. Finally, we identified the common *ITGB3* allelic variant rs15908, a silent SNP in exon 9, which significantly decreases expression of the integrin $\beta3$ subunit in homozygotes without generating a thrombocytopathic phenotype.

Many previous studies have demonstrated that several integrin subunits (eg, $\beta1$, $\beta3$, $\beta5$, $\beta8$, and αv) localize to neuronal post-synaptic densities in hippocampal neurons (Nishimura *et al*, 1998; Chan *et al*, 2003; Kramar *et al*, 2003; Chan *et al*, 2006; Pozo *et al*, 2012). However, few have examined their potential to localize to presynaptic membranes within neurotransmitter-specific projections. Immunofluorescent microscopy and subcellular fractionation analysis of the distribution of integrin $\beta3$ subunits in adult mouse midbrains revealed that integrin $\alpha v\beta3$ receptors are expressed in a subpopulation of presynaptic terminals of serotonergic neurons. Interestingly, structured illumination microscopy revealed instances whereby an $\alpha v\beta3$ receptor and SERT molecule co-localized within subcellular compartments, suggesting they may participate in a multiprotein complex, akin to the αIIb$\beta3$ SERT complexes observed in platelets (Carneiro *et al*, 2008).

In the periphery, integrin $\alpha v\beta3$ plays a pivotal role in the modulation of intracellular signaling initiated by several receptor systems, including GPCRs, RTKs, and ionotropic receptors. To date, few studies have dissected the signaling pathways influenced by $\alpha v\beta3$ signaling in neurons, but several canonical pathways typically associated with integrin engagement and clustering could potentially modulate SERT activity. One such candidate, the p38 MAPK pathway, is activated by integrin-linked kinase downstream of $\alpha v\beta3$ and can modulate SERT's catalytic activity in a manner independent of changes in SERT trafficking (Zhu *et al*, 2005; Wang *et al*, 2010; Chang *et al*, 2012; Yu *et al*, 2014). However, attempts to activate p38 MAPK with anisomycin failed to rescue the phenotype observed in $Itgb3^{+/-}$ (data not shown). On the other hand, $\alpha v\beta3$ receptors may regulate SERT activity via a mobility-mediated mechanism. In glycinergic synapses, the disruption of actin filaments dramatically alters integrin $\alpha v\beta3$-mediated modulation of glycine receptor movement (Charrier *et al*, 2010). Similarly, the actin cytoskeleton has been shown to restrict the lateral diffusion of SERTs at the plasma membrane of serotonergic synapses, which correlates with reduced 5-HT uptake (Chang *et al*, 2012). Future studies should clarify the extent to which a signaling-based and/or mobility-based mechanism of SERT regulation is employed by $\alpha v\beta3$ receptors in serotonergic synapses of the midbrain.

Despite their efficacy in treating several neuropsychiatric diseases, SSRIs fail to sufficiently address symptoms in approximately two-thirds of patients (Katzman, 2009; Kennedy *et al*, 2009; Montgomery *et al*, 2011). Our studies on *Itgb3* have revealed that a reduction in integrin $\beta3$ subunit expression is sufficient to decrease the effective dose of acutely administered citalopram and paroxetine in adult

mice, as measured by TSTs; thus implicating a deterministic role for *ITGB3* polymorphisms in the response of human patients to SSRIs. The TST has been widely used to predict antidepressant response in rodents, and we have modified the behavior to prevent C57BL/6 mice from climbing their tail, a major disadvantage of the test (Cryan *et al*, 2005). Complementary studies in other behavioral tests, such as the FST, were complicated by a severe response of $Itgb3^{+/-}$ mice to either the intraperitoneal injections or the hypothermic exposure of the test (data not shown). The reduced 5-HT binding in plasma membranes isolated from $Itgb3^{+/-}$ synaptosomes indicates that fewer SERT molecules are catalytically able to actively transport 5-HT; suggesting that lower doses of SSRIs can antagonize the remaining active SERT molecules. Our immunolocalization studies support the notion that $\alpha v\beta 3$ receptors specify a subpopulation of SERT molecules that may represent the main target of SSRIs, losing complete catalytic function in the absence of $\alpha v\beta 3$ receptors. Ascertaining if the $\alpha v\beta 3$-expressing serotonergic synapses are common to all serotonergic neurons or are derived from a subpopulation of serotonergic neurons could further our understanding of neuropsychiatric disease states (Hale *et al*, 2012).

The human *ITGB3* locus has been extensively characterized in the context of thrombosis and, more recently, autism, leading to the validation of over 1,500 variants (NCBI, dbSNP, validated by 1000 Genomes). The prevalence of patients who are antidepressant partial-responders or non-responders warrants a further look at *ITGB3* polymorphisms as they relate to neuropsychiatric disorders, especially since common variants (including rs15908, which we identified here) as well as rare loss-of-function variants in *ITGB3* are observed in humans. Future studies should aim to determine if carriers of human *ITGB3* coding variants demonstrate altered risk for neuropsychiatric disorders commonly associated with dysfunction in 5-HT as well as altered SSRI effectiveness in the treatment of various neuropsychiatric diseases. The predictive value of the TST is somewhat limited, and may reflect changes occurring in the early stages of antidepressant treatment, such as fear perception (Harmer *et al*, 2003). Given that the complexity of neural circuitry appears to be a reflection of synaptic diversity, characterizing the molecular differences between populations of $\alpha v\beta 3$-expressing and non-$\alpha v\beta 3$-expressing serotonergic synapses could advance the development of novel, more efficacious antidepressants.

FUNDING AND DISCLOSURE

NARSAD YI AWARD (AMDC), MH090256 (AMDC), MH081066 (JV-VW), Vanderbilt Postdoctoral Training Grant in Functional Neurogenomics (T32-MH65215) (MM). Human platelet western blots were funded in part by a grant from the Vanderbilt CTSA (UL1TR000445, KL2TR000446, and TL1TR000447). JV-VW has consulted with Roche, Novartis, and SynapDx and has received research funding from Roche, Novartis, SynapDx, Seaside Therapeutics, Forest, and Sunovion for unrelated work. The authors declare that over the past 3 years EHJC has received compensation from Seaside Therapeutics for consultation and support of clinical trial research that is unrelated to the work covered in the submission.

ACKNOWLEDGMENTS

We would like to acknowledge Jon Allison for general administration and organization of the Vanderbilt Murine Neurobehavioral core, and Jennifer Schafer for assistance with the super resolution microscopy. We also thank Michael Dohn for animal husbandry, general laboratory administration, and assistance with editing of the manuscript.

REFERENCES

Arai R, Karasawa N, Kurokawa K, Kanai H, Horiike K, Ito A (2002). Differential subcellular location of mitochondria in rat serotonergic neurons depends on the presence and the absence of monoamine oxidase type B. *Neuroscience* **114**: 825–835.

Askenazy F, Candito M, Caci H, Myquel M, Chambon P, Darcourt G *et al* (1998). Whole blood serotonin content, tryptophan concentrations, and impulsivity in anorexia nervosa. *Biol Psychiatry* **43**: 188–195.

Blakely RD, Ramamoorthy S, Schroeter S, Qian Y, Apparsundaram S, Galli A *et al* (1998). Regulated phosphorylation and trafficking of antidepressant-sensitive serotonin transporter proteins. *Biol Psychiatry* **44**: 169–178.

Carneiro AM, Cook EH, Murphy DL, Blakely RD (2008). Interactions between integrin alphaIIbbeta3 and the serotonin transporter regulate serotonin transport and platelet aggregation in mice and humans. *J Clin Invest* **118**: 1544–1552.

Carter MD, Shah CR, Muller CL, Crawley JN, Carneiro AM, Veenstra-VanderWeele J (2011). Absence of preference for social novelty and increased grooming in integrin beta3 knockout mice: initial studies and future directions. *Autism Res* **4**: 57–67.

Chan CS, Weeber EJ, Kurup S, Sweatt JD, Davis RL (2003). Integrin requirement for hippocampal synaptic plasticity and spatial memory. *J Neurosci* **23**: 7107–7116.

Chan CS, Weeber EJ, Zong L, Fuchs E, Sweatt JD, Davis RL (2006). Beta 1-integrins are required for hippocampal AMPA receptor-dependent synaptic transmission, synaptic plasticity, and working memory. *J Neurosci* **26**: 223–232.

Chang JC, Tomlinson ID, Warnement MR, Ustione A, Carneiro AM, Piston DW *et al* (2012). Single molecule analysis of serotonin transporter regulation using antagonist-conjugated quantum dots reveals restricted, p38 MAPK-dependent mobilization underlying uptake activation. *J Neurosci* **32**: 8919–8929.

Charrier C, Machado P, Tweedie-Cullen RY, Rutishauser D, Mansuy IM, Triller A (2010). A crosstalk between beta1 and beta3 integrins controls glycine receptor and gephyrin trafficking at synapses. *Nat Neurosci* **13**: 1388–1395.

Chavis P, Westbrook G (2001). Integrins mediate functional pre- and postsynaptic maturation at a hippocampal synapse. *Nature* **411**: 317–321.

Cingolani LA, Thalhammer A, Yu LM, Catalano M, Ramos T, Colicos MA *et al* (2008). Activity-dependent regulation of synaptic AMPA receptor composition and abundance by beta3 integrins. *Neuron* **58**: 749–762.

Cleare AJ (1997). Reduced whole blood serotonin in major depression. *Depress Anxiety* **5**: 108–111.

Cook EH, Leventhal BL (1996). The serotonin system in autism. *Curr Opin Pediatr* **8**: 348–354.

Coutinho AM, Sousa I, Martins M, Correia C, Morgadinho T, Bento C *et al* (2007). Evidence for epistasis between SLC6A4 and ITGB3 in autism etiology and in the determination of platelet serotonin levels. *Hum Genet* **121**: 243–256.

Cross S, Kim SJ, Weiss LA, Delahanty RJ, Sutcliffe JS, Leventhal BL *et al* (2008). Molecular genetics of the platelet serotonin system in first-degree relatives of patients with autism. *Neuropsychopharmacology* **33**: 353–360.

Cryan JF, Mombereau C, Vassout A (2005). The tail suspension test as a model for assessing antidepressant activity: review of pharmacological and genetic studies in mice. *Neurosci Biobehav Rev* **29**: 571–625.

DeLisi LE, Neckers LM, Weinberger DR, Wyatt RJ (1981). Increased whole blood serotonin concentrations in chronic schizophrenic patients. *Arch Gen Psychiatry* **38**: 647–650.

Hale MW, Shekhar A, Lowry CA (2012). Stress-related serotonergic systems: implications for symptomatology of anxiety and affective disorders. *Cell Mol Neurobiol* **32**: 695–708.

Hammock E, Veenstra-VanderWeele J, Yan Z, Kerr TM, Morris M, Anderson GM *et al* (2012). Examining autism spectrum disorders by biomarkers: example from the oxytocin and serotonin systems. *J Am Acad Child Adolesc Psychiatry* **51**: 712–721 e711.

Harmer CJ, Bhagwagar Z, Perrett DI, Vollm BA, Cowen PJ, Goodwin GM (2003). Acute SSRI administration affects the processing of social cues in healthy volunteers. *Neuropsychopharmacology* **28**: 148–152.

Henry LK, Field JR, Adkins EM, Parnas ML, Vaughan RA, Zou MF *et al* (2006). Tyr-95 and Ile-172 in transmembrane segments 1 and 3 of human serotonin transporters interact to establish high affinity recognition of antidepressants. *J Biol Chem* **281**: 2012–2023.

Hodivala-Dilke KM, McHugh KP, Tsakiris DA, Rayburn H, Crowley D, Ullman-Cullere M *et al* (1999). Beta3-integrin-deficient mice are a model for Glanzmann thrombasthenia showing placental defects and reduced survival. *J Clin Invest* **103**: 229–238.

Katzman MA (2009). Current considerations in the treatment of generalized anxiety disorder. *CNS Drugs* **23**: 103–120.

Kennedy SH, Andersen HF, Thase ME (2009). Escitalopram in the treatment of major depressive disorder: a meta-analysis. *Curr Med Res Opin* **25**: 161–175.

Kramar EA, Bernard JA, Gall CM, Lynch G (2003). Integrins modulate fast excitatory transmission at hippocampal synapses. *J Biol Chem* **278**: 10722–10730.

Ma N, Tan LW, Wang Q, Li ZX, Li LJ (2007). Lower levels of whole blood serotonin in obsessive-compulsive disorder and in schizophrenia with obsessive-compulsive symptoms. *Psychiatry Res* **150**: 61–69.

Mayorga AJ, Dalvi A, Page ME, Zimov-Levinson S, Hen R, Lucki I (2001). Antidepressant-like behavioral effects in 5-hydroxytryptamine(1A) and 5-hydroxytryptamine(1B) receptor mutant mice. *J Pharmacol Exp Ther* **298**: 1101–1107.

Milner R, Campbell IL (2002). The integrin family of cell adhesion molecules has multiple functions within the CNS. *J Neurosci Res* **69**: 286–291.

Montgomery S, Hansen T, Kasper S (2011). Efficacy of escitalopram compared with citalopram: a meta-analysis. *Int J Neuropsychopharmacol* **14**: 261–268.

Napolioni V, Lombardi F, Sacco R, Curatolo P, Manzi B, Alessandrelli R *et al* (2011). Family-based association study of ITGB3 in autism spectrum disorder and its endophenotypes. *Eur J Hum Genet* **19**: 353–359.

Nikonenko I, Toni N, Moosmayer M, Shigeri Y, Muller D, Sargent Jones L (2003). Integrins are involved in synaptogenesis, cell spreading, and adhesion in the postnatal brain. Brain research. *Dev Brain Res* **140**: 185–194.

Nishimura SL, Boylen KP, Einheber S, Milner TA, Ramos DM, Pytela R (1998). Synaptic and glial localization of the integrin alphavbeta8 in mouse and rat brain. *Brain Res* **791**: 271–282.

Nurden AT, Fiore M, Nurden P, Pillois X (2011). Glanzmann thrombasthenia: a review of ITGA2B and ITGB3 defects with emphasis on variants, phenotypic variability, and mouse models. *Blood* **118**: 5996–6005.

Phillips GR, Huang JK, Wang Y, Tanaka H, Shapiro L, Zhang W *et al* (2001). The presynaptic particle web: ultrastructure, composition, dissolution, and reconstitution. *Neuron* **32**: 63–77.

Pozo K, Cingolani LA, Bassani S, Laurent F, Passafaro M, Goda Y (2012). beta3 integrin interacts directly with GluA2 AMPA receptor subunit and regulates AMPA receptor expression in hippocampal neurons. *Proc Natl Acad Sci USA* **109**: 1323–1328.

Pozzi A, Zent R (2003). Integrins: sensors of extracellular matrix and modulators of cell function. *Nephron Exp Nephrol* **94**: e77–e84.

Ramaiya A, Johnson JH, Karnes HT (1997). Evaluation of the neuropharmacodynamics of paroxetine *in vivo* utilizing microdialysis. *J Pharm Sci* **86**: 1497–1500.

Ruhe HG, Mason NS, Schene AH (2007). Mood is indirectly related to serotonin, norepinephrine and dopamine levels in humans: a meta-analysis of monoamine depletion studies. *Mol Psychiatry* **12**: 331–359.

Verkes RJ, Hengeveld MW, van der Mast RC, Fekkes D, van Kempen GM (1998). Mood correlates with blood serotonin, but not with glucose measures in patients with recurrent suicidal behavior. *Psychiatry Res* **80**: 239–248.

Wang R, Li ZQ, Han X, Li BL, Mi XY, Sun LM *et al* (2010). Integrin beta3 and its ligand regulate the expression of uPA through p38 MAPK in breast cancer. *APMIS* **118**: 909–917.

Weiss LA, Kosova G, Delahanty RJ, Jiang L, Cook EH, Ober C *et al* (2006a). Variation in ITGB3 is associated with whole-blood serotonin level and autism susceptibility. *Eur J Hum Genet* **14**: 923–931.

Weiss LA, Ober C, Cook EH Jr (2006b). ITGB3 shows genetic and expression interaction with SLC6A4. *Hum Genet* **120**: 93–100.

Weiss LA, Veenstra-Vanderweele J, Newman DL, Kim SJ, Dytch H, McPeek MS Jr *et al* (2004). Genome-wide association study identifies ITGB3 as a QTL for whole blood serotonin. *Eur J Hum Genet* **12**: 949–954.

Whyte A, Jessen T, Varney S, Carneiro AM (2014). Serotonin transporter and integrin beta 3 genes interact to modulate serotonin uptake in mouse brain. *Neurochem Int* **73**: 122–126.

Wulsin LR, Musselman D, Otte C, Bruce E, Ali S, Whooley MA (2009). Depression and whole blood serotonin in patients with coronary heart disease from the Heart and Soul Study. *Psychosom Med* **71**: 260–265.

Yu L, Yuan X, Wang D, Barakat B, Williams ED, Hannigan GE (2014). Selective regulation of p38beta protein and signaling by integrin-linked kinase mediates bladder cancer cell migration. *Oncogene* **33**: 690–701.

Zhu CB, Blakely RD, Hewlett WA (2006). The proinflammatory cytokines interleukin-1beta and tumor necrosis factor-alpha activate serotonin transporters. *Neuropsychopharmacology* **31**: 2121–2131.

Zhu CB, Carneiro AM, Dostmann WR, Hewlett WA, Blakely RD (2005). p38 MAPK activation elevates serotonin transport activity via a trafficking-independent, protein phosphatase 2A-dependent process. *J Biol Chem* **280**: 15649–15658.

Zhu CB, Hewlett WA, Feoktistov I, Biaggioni I, Blakely RD (2004). Adenosine receptor, protein kinase G, and p38 mitogen-activated protein kinase-dependent up-regulation of serotonin transporters involves both transporter trafficking and activation. *Mol Pharmacol* **65**: 1462–1474.

Zhu CB, Lindler KM, Owens AW, Daws LC, Blakely RD, Hewlett WA (2010). Interleukin-1 receptor activation by systemic lipopolysaccharide induces behavioral despair linked to MAPK regulation of CNS serotonin transporters. *Neuropsychopharmacology* **35**: 2510–2520.

Supplementary Information accompanies the paper on the Neuropsychopharmacology website (http://www.nature.com/npp)